Proceedings of the Indian National Science Academy (2025) 91:1012–1021
https://doi.org/10.1007/s43538-025-00392-4

RESEARCH PAPER

Chaos phenomena in nonlinear vibration of cantilever beam with concentrated mass under the effect of fluid flow

Gaoxing Zhu[1] · Gangying Zhu[2]

Received: 25 July 2024 / Accepted: 14 January 2025 / Published online: 1 February 2025
© Indian National Science Academy 2025

Abstract
The beam model is widely used in the study of maritime structures, including columns, oil platforms, and towers surrounded by water. These structures often support concentrated masses, making it critical to understand their response amplitudes during the design phase. This paper investigates a nonlinear cantilever beam immersed in a fluid, subjected to a concentrated mass and harmonic water flow. Three nonlinear terms, spanning the first four modes, are incorporated into the analysis of the response, which is calculated using the harmonic balancing technique. Using analytical methods to analyze the frequency response, jump phenomena are identified within the triple response region between bifurcation points. This jumping behavior manifests as softening in the second, third, and fourth modes, while the first mode exhibits hardening behavior. Each nonlinear term uniquely influences the system's vibrational behavior and affects the onset of jump phenomena. Furthermore, the system temporal response, Poincaré mapping, and state-space behavior reveal distinct stability points along the phase curve. The study also explores chaos phenomena in the nonlinear beam, highlighting chaotic behavior at bifurcation points, with the geometric nonlinear term exerting the most significant impact on response irregularity. Key contributions of this research include the investigation of jump phenomena using both analytical and numerical methods, validation of findings through comparative analysis, examination of jump phenomena across the first four modes, and a comprehensive exploration of nonlinear phenomena. These phenomena encompass bifurcation and chaos, analyzed through phase curves, time responses, and Poincaré mapping. These advancements contribute to a deeper understanding of nonlinear immersed beam dynamics within the field.

Keywords Nonlinear vibration · Chaos phenomena · Cantilever beam · Immersed beams

Introduction

In the standard analysis of vibrations, the governing equations of a system are often assumed to be linear under specific excitations. However, the dynamic and vibrational behavior of most systems is inherently nonlinear. Nonlinear systems exhibit phenomena that are not present in their linear counterparts (Hoseinzadeh et al. 2023; Rezaee and Maleki 2024; Khosravi and Goudarzi 2023). Among these, the cantilever beam has garnered significant attention from researchers due to its wide range of applications (Rezaee and Arab Maleki 2013, 2019). Cantilever beams subjected to substantial excitations, such as wind and wave forces (Javanshir et al. 2015; Javanshir and Zarepour 2021), are commonly used to model various structures, including tall buildings, towers, machinery components, water tanks (Khosravi et al. 2024, 2021), oil-loading platforms, bridge piers, airplanes, spacecraft, and more (Khosravi et al. 2021; Pourreza et al. 2022; Nasrabadi et al. 2022).

Many researchers have investigated the response of nonlinear beams under certain excitation. Sapountzakis et al. (Sapountzakis and Dikaros 2011) derived the partial differential equation of a 3D uniaxial nonlinear beam under extensive excitation with the method of Hamilton's principle. Also, they determined the influence of nonlinear terms on the dynamics of a single beam under extended sinusoidal load. Li et al. (Li et al. 2021) obtained the partial differential equation of the nonlinear beam with a concentrated mass by the Euler–Bernoulli theory. Also, they determined the solution of the beam governing equation under parametric

✉ Gaoxing Zhu
zhugaoxing@126.com

[1] Jiangxi Teachers College, Yingtan 335000, Jiangxi, China

[2] Guixi No. 3 Middle School, Guixi 335400, Jiangxi, China

excitation with an analytical method and compared it with the empirical method, where the obtained results were in good agreement. Painter et al. (Painter and Amabili 2023) considered the nonlinear responses of cantilever beams under parametric excitation using time-scale and Galerkin methods. They showed that the geometric nonlinear term has a hardening effect, while the inertial nonlinear term has a softening effect on the behavior of the beam. Qaisia et al. (Al-Qaisia et al. 2000) studied the steady-state dynamics of a narrow immersed beam with concentrated mass under certain excitation. They determined the frequency response of the steady state in the first 2 main modes using the harmonic balance method. Also, Qaisia and Hamdan (Al-Qaisia and Hamdan 2002) investigated the phenomena of jump and bifurcation. Farokhi et al. (Farokhi and Erturk 2021) studied a highly flexible cantilever beam using the weighted residual method, the Galerkin method the Newmark technique, and an iterative process. Sobamowo et al. (Sobamowo et al. 2020) analyzed the jump and bifurcation phenomena on a nonlinear cantilever beam using the harmonic balance method. Wang et al. (Wang et al. 2020) examined the nonlinear dynamics of a suspended cantilever beam under the influence of gravity. Gelerkin and linear mode shape methods were used to derive the nonlinear equation governing the nonlinear beam vibrations. They used the time-scale method to solve the governing equations of the system, and investigated nonlinear phenomena including jump in the first 2 modes. They showed that the jump curve is softening in the second mode. Also, the study of the phase curve demonstrated that the system is of the limit cycle type. Therefore, there will be only 1 point on the Poincaré map. Philip et al. (Philip et al. 2023) examined the effects of a nonlinear energy sink in order to reduce the vibration of a pipe transporting fluid under the effect of an external harmonic excitation. The pipe was modeled via the Euler–Bernoulli beam theory, and the nonlinear energy sink has nonlinear stiffness and linear damping. Increasing the fluid velocity reduces the steady-state response amplitude, and expands the unstable response region. Their results showed that the middle of the pipe is the best position for connecting the nonlinear energy sink to a curved pipe transmitting fluid under the external excitation. Sarvi (Sarvi 2021) analyzed the phenomenon of random jump in a nonlinear cantilever beam submerged in water. They showed that the jump phenomenon in the first mode is of hardening type. To verify the accuracy of results, they used the 4th-order Runge–Kutta numerical method. The dynamic stability and vibration behavior of small-scale axially moving beams on a viscoelastic basis in a heat-humidity environment were analyzed by Sarparast et al. (Sarparast et al. 2020). Their study provides valuable insights and a modeling approach that can be leveraged for designing and enhancing the performance of nonlinear vibration absorbers for submarine structures.

In this study, we investigate the nonlinear dynamic behavior of a cantilever beam with a concentrated mass, submerged in fluid and subjected to harmonic water flow. The model is developed based on large deformation theory with the inextensibility constraint for the beam, an assumption widely applicable to engineering structures. Notably, we employ finite strain theory to derive the Green–Lagrange strain tensor parameters specifically for the Euler–Bernoulli beam model, marking the first application of this approach in such a context. This formulation enables the capture of potential energy variations in the beam by incorporating Green–Lagrange strain tensor parameters, which account for all nonlinear terms, thereby adhering to finite strain assumptions. To derive the governing equations of motion and apply the appropriate boundary conditions for a slender beam partially immersed in fluid, the model incorporates three nonlinear terms alongside fluid flow effects. Using the harmonic balance technique, we analyze the system's frequency and force responses, uncovering a jump phenomenon in both. In the frequency response, bifurcation points emerge, exhibiting a triple response characteristic. Similarly, the force response curve suggests the presence of potential chaotic behavior in the beam. We validate the analytical solutions through numerical simulations conducted with MatCont software, demonstrating excellent agreement between the frequency and force responses. This methodology emphasizes intricate nonlinear effects, such as bifurcations and chaotic dynamics, providing new insights into fluid–structure interaction models for submerged beams in oscillatory flows.

Governing equations of motion

The studied cantilever beam, whose nonlinearity is caused by the geometry of the beam, is shown in Fig. 1. The depth of the fluid is denoted by l_1, and the concentrated mass is denoted by M, which is placed at a distance d from the end of the beam. The purpose of designing and building columns, oil platforms, and structures immersed in water is to bear the load caused by concentrated mass. Therefore, in order to adapt the studied model to reality, the immersed beam is studied considering the concentrated mass. Since the beam's thickness is anticipated to be extremely thin in relation to its length, its torsional inertia and shear deformation can be disregarded.

In this study, we assume the in-extensibility condition for the beam, which means that any longitudinal displacement along the beam's length is negligible. This assumption allows us to focus exclusively on transverse displacements and vibrations, in line with the principles of the Euler–Bernoulli beam theory. By discarding longitudinal displacement, we simplify the model to capture the

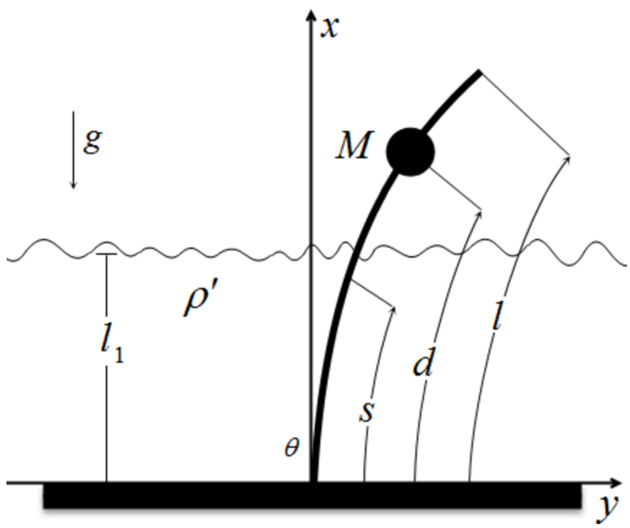

Fig. 1 Cantilever beam with concentrated mass under fluid flow excitation

primary nonlinear behaviors of interest in the transverse direction. Discarding the longitudinal displacement, the displacement fields will be as:

$$U(x,z,t) = -z\frac{\partial w(x,t)}{\partial t}, \qquad W(x,z,t) = w(x,t) \tag{1}$$

where U and W are displacement in x and y directions, and t is time.

In deriving the governing equations for the Euler–Bernoulli beam model, we employed the second Piola–Kirchhoff stress tensor and the Green–Lagrange strain tensor under finite strain assumptions. The Green–Lagrange strain tensor is particularly well-suited for capturing large strain behavior, as it provides a measure of strain that remains valid under nonlinear deformations. According to Lurie (Lurie 2010), this formulation enables a more accurate representation of strain in cases of significant deformation. Using finite strain theory, we derive the first parameter of the Green–Lagrange strain tensor by substituting the Euler–Bernoulli assumptions, which simplify the strain tensor components to reflect bending-dominated deformations. The resulting expression for this parameter is as follows:

$$E_{xx} = \frac{1}{2}z^2\left(\frac{\partial^2 w}{\partial x^2}\right)^2 - z\frac{\partial^2 w}{\partial x^2} + \frac{1}{2}\left(\frac{\partial w}{\partial x}\right)^2 \tag{2}$$

This formulation facilitates the accurate modeling of the beam's deformation by incorporating both the geometrical nonlinearities inherent in large strain conditions and the material response. This approach represents a more generalized form of the Euler–Bernoulli beam model, accommodating scenarios where finite strain effects are non-negligible.

Due to the presence of fluid and concentrated mass on the beam, kinetic energy variations can be calculated as follows:

$$\delta T = \frac{1}{2}\rho A\left(1 + C_m K_m\right)\int_0^{l_1}\delta\left(\dot{U}^2 + \dot{W}^2\right)ds + \frac{1}{2}\rho A\int_{l_1}^{l}\delta\left(\dot{U}^2 + \dot{W}^2\right)ds + \frac{1}{2}M\delta\left(\dot{U}^2 + \dot{W}^2\right)_{s=d} \tag{3}$$

in which, C_m is the inertia of added mass, K_m is the fluid density ratio, ρ is density, A is area, d is location of concentrated mass.

Also, using the Green–Lagrange tensor, the variation of beam strain energy is obtained as:

$$\begin{aligned}\delta V &= \int_V \sigma_{xx}\delta E_{xx}dV_0 \\ &= \int_0^L\int_A \sigma_{xx}\left(z^2\frac{\partial^2 w}{\partial x^2}\frac{\partial^2 \delta w}{\partial x^2} - z\frac{\partial^2 \delta w}{\partial x^2} + \frac{\partial w}{\partial x}\frac{\partial \delta w}{\partial x}\right)dAdx\end{aligned} \tag{4}$$

in which σ_{xx} is axial stress. By using Hamilton's principle, the equation governing the transverse vibrations of a nonlinear cantilever beam with a concentrated mass under extensive excitation can be obtained as the following:

$$\begin{aligned}&\frac{3h^5}{160}\frac{\partial^4 w}{\partial x^4}\left(\frac{\partial^2 w}{\partial x^2}\right)^2 + \frac{h^3}{24}\frac{\partial^4 w}{\partial x^4}\left(\frac{\partial w}{\partial x}\right)^2 + \frac{h^3}{12}\frac{\partial^4 w}{\partial x^4} + \frac{6h^5}{160}\frac{\partial^2 w}{\partial x^2}\left(\frac{\partial^3 w}{\partial x^3}\right)^2 \\ &+\frac{h^3}{24}\left(\frac{\partial^2 w}{\partial x^2}\right)^3 + \frac{h^3}{6}\frac{\partial^3 w}{\partial x^3}\frac{\partial^2 w}{\partial x^2}\frac{\partial w}{\partial x} + \frac{L^3h^4}{EI}C\frac{\partial w}{\partial t}\left(\frac{\partial^3 w}{\partial x^3}\right)^2 - \frac{3h}{2}\frac{\partial^2 w}{\partial x^2}\left(\frac{\partial w}{\partial x}\right)^2 \\ &+\frac{L^3}{EI}\left[\frac{\rho A}{2}\left(1 + C_m K_m\right)\left(1 + \left(\frac{\partial w}{\partial x}\right)^2\right) + M\delta(x-d)\right]\frac{\partial^2 w}{\partial t^2} = \frac{L^3}{EI}f(x,t)\end{aligned} \tag{5}$$

in which, EI is the flexural rigidity, $f(x,t)$ stands for the external excitation, and $C = C_s + C_f$ (N.s/m) is the damping coefficient that will make the response stable. The coefficient C represents the combined effects of various damping mechanisms, including structural (material) damping (C_s) intrinsic to the beam and additional damping induced by the interaction with the surrounding fluid (C_f). This coefficient accounts for energy dissipation within the system due to the beam's material properties and fluid–structure interactions. Also, to consider the interaction between the structure and water with specific mass ρ_f, viscosity-type damping is assumed.

In the model, the damping coefficient C captures the effects of fluid viscosity as part of the fluid–structure one-way interaction, representing the energy dissipation due to viscous resistance. This coefficient accounts for the damping influence of the surrounding fluid as the beam oscillates, and its value is determined based on fluid properties such as density and dynamic viscosity, along with the oscillation frequency. The value of C can be calibrated through empirical data for similar submerged systems or estimated using reference values from the literature. Including c provides a realistic approximation of the fluid's viscous effects on the beam's vibrational behavior.

In Eq. (5), the mass of the beam is expressed as mass per unit length, and the inertial force from the concentrated mass is represented using a Dirac delta function. The Dirac delta function, with units of 1/m, localizes the concentrated mass along the beam, ensuring that the resulting equation is in terms of force per unit length. This approach aligns with standard formulations of beam dynamics, providing an accurate representation of the combined effects of distributed mass and localized inertial forces from the concentrated mass.

The boundary conditions of the cantilever beam are as:

$$\begin{aligned} x = 0: &\quad w = w' = 0 \\ x = L: &\quad w'' = w''' = 0 \end{aligned} \tag{6}$$

Based on the Galerkin technique, the ordinary differential equation that depends only on time is obtained by using the linear mode shape of the cantilever beam. In reality, the mode shape of the beam is nonlinear, but because the nonlinear terms of the equation governing the vibrations of the beam are assumed to be weak, the linear mode shape can be used to derive the ordinary differential equation:

$$w(x,t) = \sum_{i=1}^{N} \varphi_i(x) q_i(t) \tag{7}$$

in which, $q_i\,(t)$ stands as the generalized coordinate of the system, and $\phi_i\,(x)$ remains the mode shape of the i^{th} mode of the single beam, which can be calculated from the following equation:

$$\varphi_i(x) = \cosh \beta_i x - \cos \beta_i x + \frac{\cos \beta_i l + \cosh \beta_i l}{\sin \beta_i l + \sinh \beta_i l} \left(\sin \beta_i x - \sinh \beta_i x \right) \tag{8}$$

in which, β_i are the roots of the frequency equation, and the first 4 roots are given in Table 1.

Although the nonlinearity in the system is assumed to be weak, the inclusion of nonlinear terms in the governing equation is essential to capture specific nonlinear behaviors such as bifurcation, jump phenomena, and chaos. These effects are crucial in understanding the dynamic response of the beam, especially under the influence of fluid flow and concentrated mass. Using linear mode shapes simplifies the analysis while still allowing us to investigate these nonlinear phenomena accurately. While nonlinear normal modes provide a more refined approach for strongly nonlinear systems, their application would significantly increase computational complexity. Given the weak nature of the nonlinearity in this study, linear mode shapes strike a balance between computational simplicity and analytical accuracy, effectively capturing the key nonlinear dynamics without the need for more complex nonlinear normal modes.

Table 1 Roots of the frequency equation for a cantilever beam

Model number	1	2	3	4
β	1.8751	4.6941	7.8548	10.9958

It is clear that the excitation function of the external force is also expanded based on the beam mode shape:

$$f(x,t) = \sum_{i=1}^{N} \varphi_i(x) h(t) \tag{9}$$

It is assumed that the beam is under harmonic excitation *h(t)*:

$$h(t) = F_0 \cos\left(\overline{\Omega} t\right) \tag{10}$$

In the above equation, F_0 is the constant amplitude of excitation force, and Ω is the frequency of the excitation force.

By substituting Eqs. (7) and (10) into Eq. (5) and applying the modes orthogonality, the governing equation of the system is as:

$$\ddot{q} + q + c\dot{q} + r_1 q^2 \ddot{q} + r_1 q \dot{q}^2 + r_2 q^3 = r_3 P \cos(\Omega t) \tag{11}$$

The coefficients of Eq. (11) can be calculated from Eq. (12).

$$r_1 = \frac{\alpha_3}{p^2 \alpha_1}, \quad r_2 = \frac{2\alpha_4}{p^2 \alpha_3}, \quad r_3 = \frac{p\alpha_5}{\alpha_2}, \quad P = \frac{F_0}{\rho A l^2 \gamma^2}, \quad \gamma^2 = \frac{EI}{\rho A l^2} \tag{12}$$

To solve the nonlinear equation governing the system, it is assumed that there is a phase difference in a certain excitation. Therefore, the vibration equation for a damped system can be written as:

$$\begin{aligned} \ddot{q} + q + c\dot{q} + r_1 q^2 \ddot{q} + r_1 q \dot{q}^2 + r_2 q^3 &= r_3 P \cos(\Omega t + \gamma) \\ &= a_1 \cos(\Omega t) - a_2 \sin(\Omega t) \end{aligned} \tag{13}$$

in which, a_1 and a_2 are the equivalent excitation amplitudes. It is assumed that the excitation amplitude is $P = \sqrt{a_1^2 - a_2^2}$ (Painter and Amabili 2023). As a first approximation, the following solution is considered:

$$q_1(t) = a_0 \cos(\Omega t) \tag{14}$$

Substituting Eq. (14) inside the Eq. (13) yields

$$\begin{aligned} &a_0\left(-\Omega^2 + 1\right)\cos(\Omega t) - c a_0 \Omega \sin(\Omega t) - r_1 a_0^3 \Omega^2 \cos^3(\Omega t) \\ &\quad - r_1 a_0^3 \Omega^2 \cos(\Omega t) \sin^2(\Omega t) + r_2 a_0^3 \cos^3(\Omega t) = a_1 \cos(\Omega t) - a_2 \sin(\Omega t) \end{aligned} \tag{15}$$

Using the expansion of trigonometric functions and collect harmonics, we will have:

$$\left[a_0\left(1-\Omega^2\right)+\frac{3}{4}\left(r_2a_0^3-r_1a_0^3\Omega^2\right)-\frac{1}{4}r_1a_0^3\Omega^2\right]$$
$$\cos(\Omega t)-ca_0\Omega\sin(\Omega t)$$
$$\left(\frac{1}{4}r_1a_0^3\Omega^2-\frac{1}{4}r_1a_0^3\Omega^2+\frac{1}{4}r_2a_0^3\right)\cos(3\Omega t) \tag{16}$$
$$=a_1\cos(\Omega t)-a_2\sin(\Omega t)$$

and quating coefficients of first harmonics and balance the harmonics (Krack and Gross 2019), the frequency response of the cantilever beam is obtained as:

$$\left[\left(1-\Omega^2\right)a_0+\left(\frac{3}{4}r_2-r_1\Omega^2\right)a_0^3\right]^2+\left(a_0c\Omega\right)^2=P^2 \tag{17}$$

The nonlinear oscillators studied by Al-Qaisia and Hamdan (Al-Qaisia and Hamdan 1999) are similar to Eq. (15). This formula describes the inextensible beam's nonlinear planar flexural motion, as seen in Fig. 1. In this equation, the terms r_1 and r_2 represent inertial nonlinearities stemming from the kinetic energy of axial motion. Equations (3) and (4) make use of the inextensibility condition and its derivatives, which is how they arise. The softening effect of the first nonlinear component causes the natural frequency to drop as the motion amplitude decreases. On the other hand, the second nonlinear component exhibits a hardening effect, which causes the natural frequency to rise as the vibration amplitude increases. Equation (15) last nonlinear component, r_3, is a hardening static type that results from the potential energy stored in bending and is linked to the application of nonlinear curvature. This means that 2 conflicting softening and hardening nonlinearities, which have essentially different response characteristics, control the response of the previously described nonlinear oscillator. The predominant nonlinearity that determines the response depends on the system characteristics and anticipated mode shape, as well as the relative values of coefficients r_1 and r_2 in the equation. It is expected that this oscillator's steady-state response will be of the softening type when $r_1/r_2>1.6$; if not, it will be of the hardening type. As the number of modes increases, the present problem's initial mode, $r_1/r_2<1.6$, and higher modes, $r_1/r_2>1.6$, intensify. As such, 1 anticipates that the beam response for the first mode will show a hardening feature and that the response will show a softening tendency for the second and higher modes. In the section that follows, estimates of the steady state for the first and second modes are provided and examined.

Results and discussion

To ensure reproducibility and facilitate independent validation of the results, all parameters used in the simulations are listed here. These parameters include physical properties of the beam and fluid, initial and boundary conditions, and any constants applied to account for damping, mass distribution, and fluid–structure interactions.

- **Beam properties:** Length $L=2.2$ m, cross-sectional area $A=16$ mm^2, flexural rigidity $EI=4.48$ N.m^2.
- **Concentrated mass properties:** Mass M = 0.1kg, position along the beam $d=1.6$ 5m.
- **Fluid properties:** Density $\rho_f=1000$ kg/m^3.
- **Damping coefficient:** Structural damping $C_s=1\times10^{-4}$ N.s/m, viscous damping $C_f=0.05$ N.s/m.
- **Excitation parameters:** Amplitude and frequency range of the harmonic water flow $F_0=10$ N, $\Omega=2$ Hz.

These values were chosen based on relevant experimental or literature values. This detailed parameterization allows for an accurate reproduction of our simulations and validation of the findings discussed in this study. Accordingly, the numerical values of the coefficients of Eq. (11) are demonstrated in Table 2.

Equation (15) is the frequency response resulting from the analytical solution of the harmonic balance technique, in which, the time parameter (t) is removed from the analytical response. In other words, Eq. (15) is independent of time. This equation makes it possible to study the jump phenomenon, but it has limitations and cannot be used to investigate the time response and phase curve.

The curve in Fig. 2 demonstrates the frequency response of the nonlinear beam in relation to the excitation frequency by using 2 analytical and numerical methods. The result of the analytical solution shown in Fig. 2 with a continuous line is an implicit function, which is the result of plotting Eq. (16). By directly solving the nonlinear differential equation governing the vibrations of the cantilever beam Eq. (7) using the numerical method, the response is extracted based on the excitation frequency. The comparison of the solutions obtained from the analytical and numerical solutions in Fig. 2 shows that the results are in good agreement with each other, and the maximum difference is 5%. The nonlinear jump phenomena in a cantilever beam's initial mode are seen in Fig. 2. The leap will be of the hardening kind because of the response curve's tendency toward the right side of the picture. In the hardening jump phenomenon, increasing the excitation frequency results in a downward jump (decreasing the oscillation amplitude). Conversely, decreasing the

Table 2 Coefficient of Eq. (11)

Mode	c	r_1	r_2	r_3	P
1	0.02	1.05625	0.65824	0.125	0.2
2	0.02	8.55210	1.256484	0.125	0.2
3	0.02	11.58426	2.078123	0.125	0.2

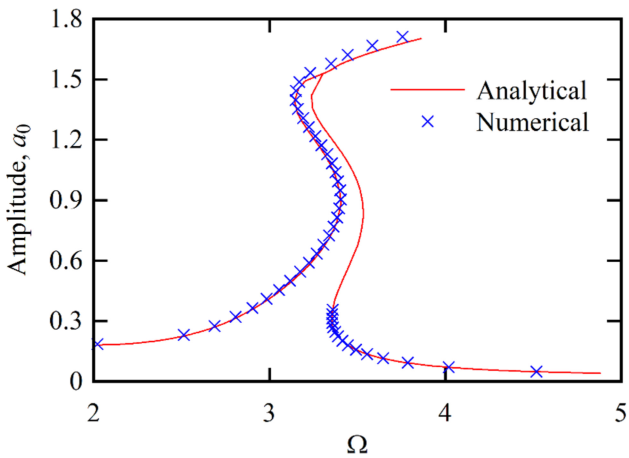

Fig. 2 Frequency response of a nonlinear beam under harmonic excitation

excitation frequency results in an upward jump (increasing the oscillation amplitude). Points 1 and 2 in Fig. 2, which show the phenomena of jumping down and up, respectively, are called bifurcation points. The area between these points is called the triple response area, and the nonlinear beam may behave chaotically in the triple response area. The curve in Fig. 2 is the solution of Eq. (7) considering that all 3 terms are nonlinear. In the following, the effect of each of the nonlinear terms will be investigated and compared with the linear state of the beam. The physical cause of the jump phenomenon is the reduction of energy at the bifurcation points. The beam tends to oscillate in a direction that has minimum energy.

The effects of nonlinear inertial and geometric parameters are compared with each other in Fig. 3. The nature of the jump phenomenon due to the nonlinear term of inertia (I) is of softening type. As seen in Fig. 3, only the nonlinear term (I) is inclined to the left. The nonlinear terms (II) and (III) which are caused by the inertial and geometrical nonlinearity, are inclined to the right side of the diagram, causing the hardening of the beam jump phenomenon. Curve (IV) shows the frequency response of the beam with 3 nonlinear terms. In other words, curve (IV) is the analytical solution of Eq. (7) which has 3 nonlinear parameters (I), (II), and (III) simultaneously. There are phenomena occurring in nonlinear systems that cannot be observed in linear systems. The curve (V) in Fig. 3 is the nonlinear frequency response without considering the nonlinear terms.

The frequency response of a nonlinear cantilever beam immersed in water is analyzed for the first four modes, as shown in Fig. 4. Unlike the first mode, where the jump phenomenon exhibits hardening characteristics, the jump phenomena in modes 2, 3, and 4 are inclined to the left, indicating softening behavior. In the softening jump phenomenon, an increase in the excitation frequency causes an upward jump, while a decrease in the excitation frequency results in a downward jump. As the mode number increases, the influence of the nonlinear inertia term (I) becomes more pronounced, which contributes to the softening nature of the jump phenomenon in modes 2, 3, and 4. Additionally, the jump phenomenon becomes progressively softer with higher beam modes. This is reflected in the increasing leftward inclination of the response curve within the triple response region as the mode number rises.

Fig. 3 Comparison between the effects of the nonlinear terms

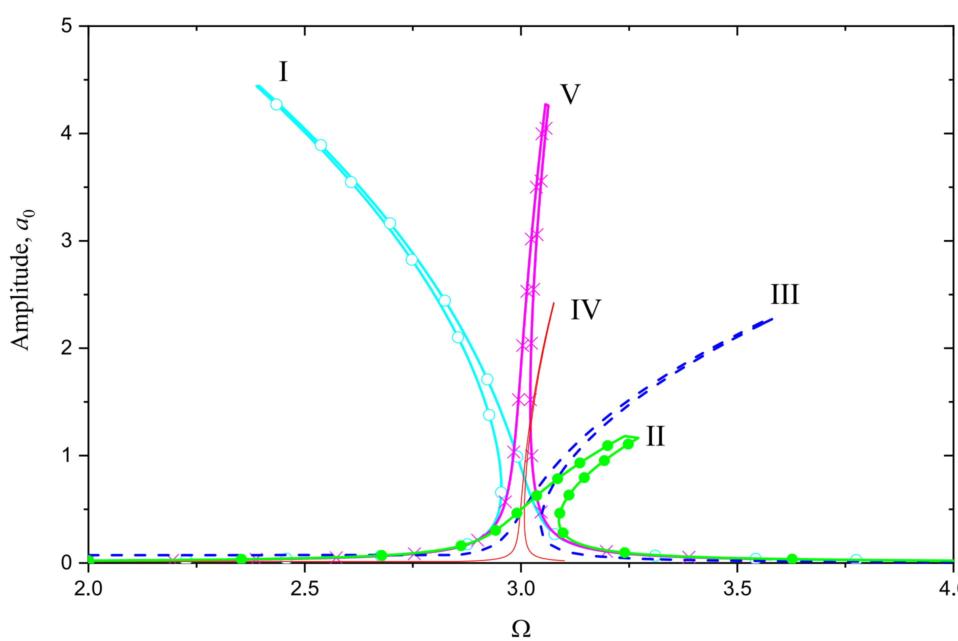

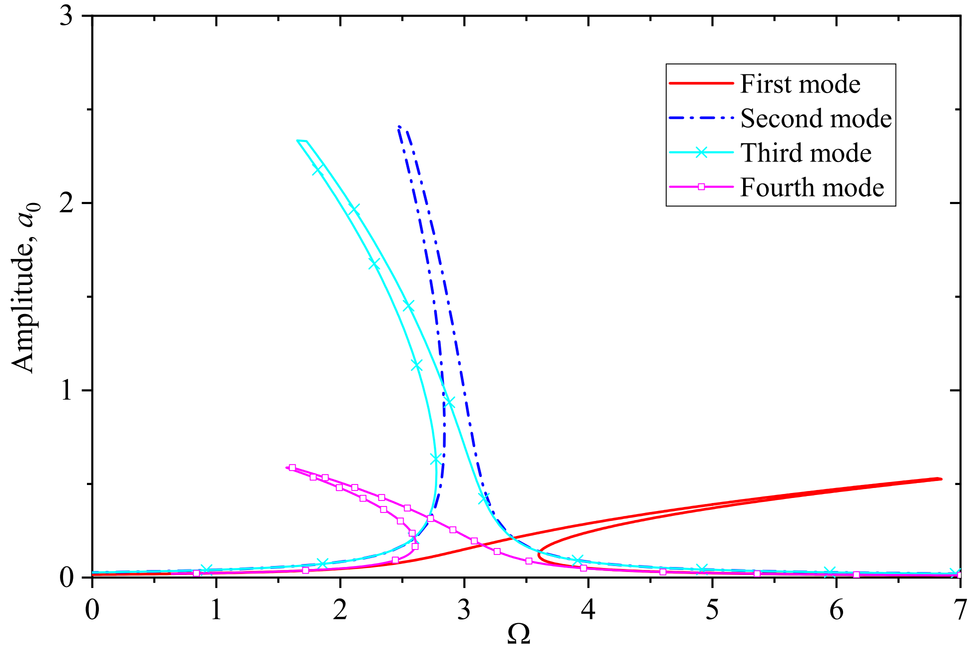

Fig. 4 Comparison between the frequency responses of the nonlinear beam in the first 4 modes

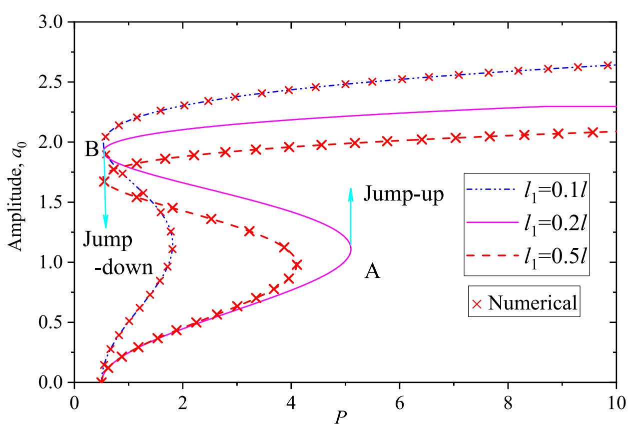

Fig. 5 Influence of fluid height and excitation force amplitude on bifurcation phenomenon in analytical and numerical solutions

In Fig. 5, we show the amplitude response between points A and B, corresponding to the region of jump-down and jump-up conditions. This region represents a saddle point in the system's dynamics, where direct numerical solutions often fail due to the instability of the saddle. To accurately capture this behavior, we used the continuation software MatCont, which is well-suited for analyzing bifurcations and tracking solutions through saddle points. MatCont allowed us to generate the bifurcation plots and numerically trace the unstable branches with precision by following the continuation path of solutions. Using MatCont, we iteratively tracked the stable and unstable branches to map out the response curve between A and B. This approach made it possible to approximate the amplitudes in the otherwise numerically unstable saddle region by employing adaptive steps and corrective algorithms within MatCont to handle the bifurcation turning points. Also, in Fig. 5, the effect of fluid height and excitation force amplitude on the bifurcation phenomenon has been investigated using analytical and numerical solutions. By increasing the excitation amplitude at point A in Fig. 5, the phenomenon of jumping up occurs, while by decreasing the excitation amplitude, the phenomenon of jumping down occurs. Therefore, $P=1.45$ is a critical point, and it is predicted that the chaos phenomenon will occur in the nonlinear beam response. The 4th-order Runge–Kutta numerical solution is not able to determine the response of the system in the triple area (the area between points 1 and 2). This method can only show the boundary of the triple response area and bifurcation points. However, by considering different initial conditions in the numerical solution method, these areas can also be identified. In Figs. 2 and 5, the comparison between the analytical and the numerical solutions shows the accuracy of the results. In Fig. 5, the numerical solution was compared with the analytical solution, where the results showed the correctness of the methods used. Now it is possible to evaluate the solution of the differential Eq. (7) with respect to time using the numerical method.

The time trace of the nonlinear beam for the first mode is examined in Fig. 6. As a result of excitation, the amplitude of oscillation increases till $t=23$s, but due to the existence of damping and nonlinear terms of inertia in Eq. (7), the amplitude of oscillation is controlled. For the numerical study of Eq. (7), all the coefficients were introduced except for the excitation frequency. For this purpose, $\Omega=3.1$, which is one of the critical points on the jump curve, was selected for all Figs. 5, 6, 7, 8, 9, 10. If the response amplitude is

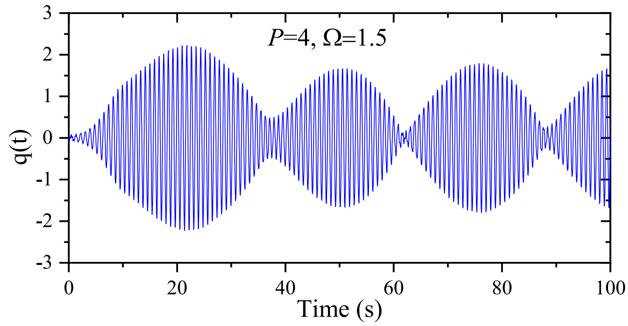

Fig. 6 Time trace of the nonlinear cantilever beam in the first case

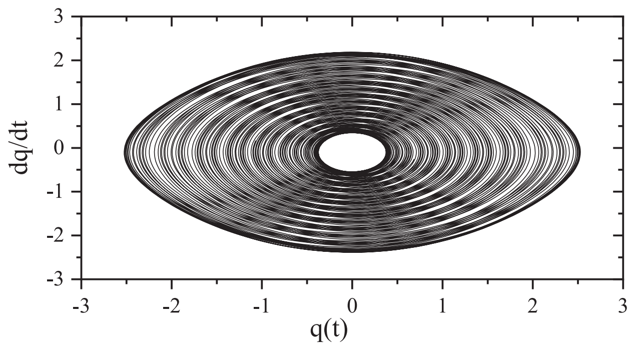

Fig. 7 The phase curve of the nonlinear beam in the first mode

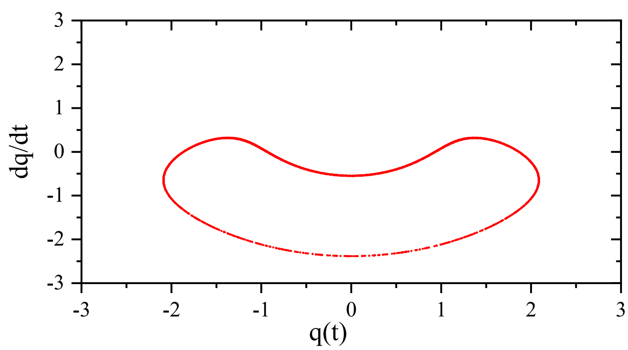

Fig. 8 The Poincaré map

investigated in relation to the response speed of the nonlinear beam, a phase plane can be seen. Comparing the behavior of the Eq. (7) system in 2 time and phase response curves can lead to a better understanding of the nonlinear phenomena of the beam.

By analyzing the phase curve behavior of a nonlinear beam with a concentrated mass subjected to fluid flow, the onset of chaos can be anticipated. Initially, the phase curve exhibits a clockwise trajectory with a decreasing amplitude. However, as the curve approaches its center, the direction of movement reverses, transitioning to a counter-clockwise

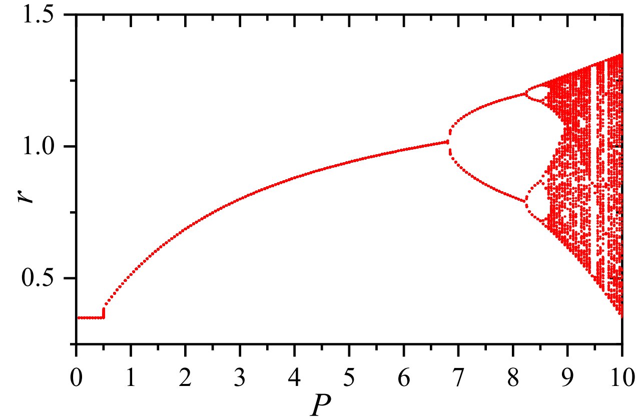

Fig. 9 Chaos phenomenon of the nonlinear beam from Eq. (7)

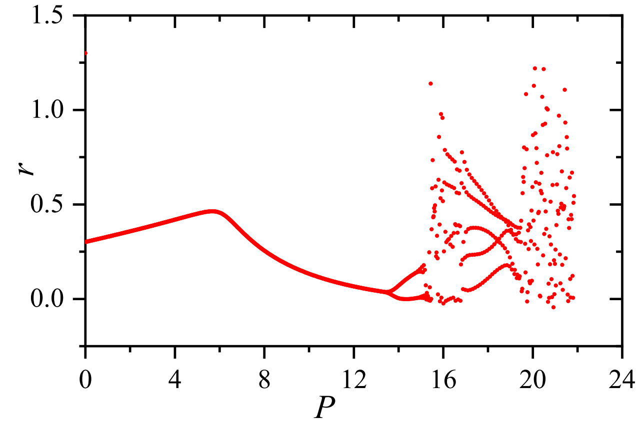

Fig. 10 Nonlinear beam chaos phenomenon from Eq. (7) without considering the nonlinear terms of inertia

trajectory. This shift in movement direction, from clockwise to counter-clockwise, indicates a potential for chaotic behavior in the system.

The point of intersection in the continuous solution of Eq. (7) in the 3D phase space with a 2D plane will show the Poincaré map. The Poincaré map in Fig. 8 can be interpreted as a discrete dynamic system with a state space that is 1D smaller than the original continuous dynamic system. The Poincaré map has also been examined in the same way as the curves of Figs. 6, 7, 8, 9, 10 at the critical excitation frequency of 3.1. The results of the Poincaré mapping show the behavior of the non-limit cycle system with countless stability points. Therefore, it is predicted that the behavior of the system will be nonlinear, irregular, and chaotic.

By assuming $r = \sqrt{q^2 - \dot{q}^2}$ and comparing r with respect to the excitation amplitude P, the chaos phenomenon can be investigated. In Fig. 9, the chaos phenomenon of the nonlinear beam has been investigated using Eq. (7). As it is seen, the behavior of this beam has been investigated up to the excitation amplitude $P = 10$. At $P = 6.8$, r enters into irregular behavior, which is called chaos phenomenon. Due to the presence of damping terms in the beam equation, the chaos in the system is controlled, so r converges at values of $P < 6.8$.

Examining the effect of each of the nonlinear terms in the solution of r reveals interesting results in the curve of the chaos phenomenon. In Fig. 10, the effect of the geometric nonlinear term r_3q^3 alone on the chaos curve is investigated (nonlinear inertia terms in Eq. (7) are omitted). As it is clear from the comparison between Fig. 10 and Fig. 9, the chaos phenomenon occurs in different excitation amplitudes. The response is convergent up to $P=13.6$. After that, the bifurcation phenomenon occurs, and this bifurcation phenomenon enters the chaos phenomenon at $P=15.2$.

Each nonlinear factor exerts a distinct influence on the frequency response, resulting in a hardening-type jump phenomenon in the first mode. In contrast, the frequency responses of the second, third, and fourth modes provide evidence of softening-type jump phenomena. The time response and phase curve of the system were analyzed at the bifurcation point, where the upward jump phenomenon occurs. Results from the Poincaré map reveal multiple stability points in the system's response. Consequently, it can be predicted that as the excitation amplitude increases, chaotic behavior will emerge in the nonlinear beam under fluid flow effects. Key innovations of this study include the investigation of upward and downward jump phenomena using both the harmonic balance technique and the fourth-order Runge–Kutta method, as well as the comparative validation of these methods. Additional contributions involve the detailed examination of jump phenomena across the first four modes and a comprehensive analysis of nonlinear behaviors, including bifurcation and chaos, through phase curves, time response, and Poincaré mapping.

Conclusion

This study introduces a novel investigation into the nonlinear dynamic behavior of a cantilever beam immersed in fluid flow and incorporating a concentrated mass. For the first time, the governing differential equations are derived using finite strain theory and the Green–Lagrange strain tensor within the Euler–Bernoulli beam framework, effectively capturing large deformation effects under the inextensibility constraint. The analysis employs the Galerkin discretization method to incorporate fluid–structure interaction terms, accounting for both inertial coupling and viscous damping. This innovative approach adds a new dimension to traditional beam analysis, providing deeper insights into the complex dynamics of submerged structures.

The application of the harmonic balance technique in this study represents a significant contribution to the analysis of bifurcation and jump phenomena in both frequency and force response curves. The findings reveal a hardening-type jump in the primary mode, contrasted with softening-type jumps in higher modes, offering new insights into mode-specific behaviors under nonlinear conditions. This differentiation, not previously addressed in the literature, highlights the unique influence of nonlinear geometric terms on chaotic responses in submerged beams. Additionally, the observed Poincaré stability points indicate that increasing the excitation amplitude could trigger chaotic dynamics—a prediction rarely explored in prior fluid–structure interaction models. These results advance the understanding of nonlinear dynamics in submerged structures and underscore the critical role of mode-specific nonlinearities in predicting complex vibrational behavior.

In conclusion, the innovative integration of finite strain theory, nonlinear geometric effects, and fluid–structure interaction into the analysis of cantilever beam dynamics significantly advances the understanding of chaotic behavior in fluid-driven systems. These findings pave the way for improved prediction and control of complex behaviors in engineering applications involving submerged structures.

Author contributions All authors contributed to the study's conception and design. Data collection, simulation and analysis were performed by" Gaoxing Zhu and Gangying Zhu ". Also, the first draft of the manuscript was written by Gaoxing Zhu. Gangying Zhu commented on previous versions of the manuscript.

Data availability The authors do not have permission to share data.

Declarations

Conflicts of interest The authors declare no competing interests.

References

Al-Qaisia, A., Hamdan, M.: On the steady state response of oscillators with static and inertia non-linearities. J. Sound Vib. **223**(1), 49–71 (1999)

Al-Qaisia, A., Hamdan, M.: Bifurcations and chaos of an immersed cantilever beam in a fluid and carrying an intermediate mass. J. Sound Vib. **253**(4), 859–888 (2002)

Al-Qaisia, A., Hamdan, M., Al-Bedoor, B.: On the steady state response of a cantilever beam partially immersed in a fluid and carrying an intermediate mass. Shock. Vib. **7**(4), 179–194 (2000)

Farokhi, H., Erturk, A.: Three-dimensional nonlinear extreme vibrations of cantilevers based on a geometrically exact model. J. Sound Vib. **510**, 116295 (2021)

Hoseinzadeh, M., Pilafkan, R., Maleki, V.A.: Size-dependent linear and nonlinear vibration of functionally graded CNT reinforced imperfect microplates submerged in fluid medium. Ocean Eng. **268**, 113257 (2023)

Javanshir, I., Zarepour, G.: Vibration analysis of fluid-structure interaction using tuned mass dampers. J. Appl. Eng. Sci. **19**(2), 318–326 (2021)

Javanshir, I., Javanshir, N., Barmaki, R., Mahmoodi, M.: Modeling of the fluid-induced vibrations in sliding gate dams. J. Vibroeng. **17**(1), 478–486 (2015)

Khosravi, S., Goudarzi, M.A.: Seismic risk assessment of on-ground concrete cylindrical water tanks. Innov. Infrastruct. Solut. **8**(1), 68 (2023)

Khosravi, S., Yousefi, M.M., Goudarzi, M.: Development of seismic fragility curves of cylindrical concrete tanks using nonlinear analysis. Amirkabir J. Civil Eng. **53**(1), 71–88 (2021)

Khosravi, S., Amirsardari, S., Goudarzi, M.A.: Dynamic behavior of rectangular tanks with limited freeboard under seismic loads: experimental, analytical and machine learning investigations. J. Press. Vessel Technol. **23**, 1 (2024)

Krack, M. and J. Gross, *Harmonic balance for nonlinear vibration problems*. 2019, Springer. P. 1–10

Li, B., Hu, K., Jin, G., Song, Y., Ge, G.: Response of cantilever model with inertia nonlinearity under transverse basal Gaussian colored noise excitation. Math. Probl. Eng. **2021**, 1–9 (2021)

Lurie, A.I., *Theory of elasticity*. 2010: Springer Science & Business Media.

Nasrabadi, M., Sevbitov, A.V., Maleki, V.A., Akbar, N., Javanshir, I.: Passive fluid-induced vibration control of viscoelastic cylinder using nonlinear energy sink. Mar. Struct. **81**, 103116 (2022)

Painter, B., Amabili, M.: Non-planar vibrations of beams with geometric imperfections and hysteretic boundary conditions. Nonlinear Dyn. **111**(21), 19749–19761 (2023)

Philip, R., Santhosh, B., Balaram, B., Awrejcewicz, J.: Vibration control in fluid conveying pipes using NES with nonlinear damping. Mech. Syst. Signal Process. **194**, 110250 (2023)

Pourreza, T., Alijani, A., Maleki, V.A., Kazemi, A.: The effect of magnetic field on buckling and nonlinear vibrations of graphene nanosheets based on nonlocal elasticity theory. Int. J. Nano Dimens **13**(1), 54–70 (2022)

Rezaee, M., Arab Maleki, V.: A new analytical method to investigate the vibrational behavior of fluid embedded pipe. Iran. J. Mech. Eng. Trans. ISME **15**(1), 6–20 (2013)

Rezaee, M., Arab Maleki, V.: Passive vibration control of the fluid conveying pipes using dynamic vibration absorber. Amirkabir J. Mech. Eng. **51**(3), 111–120 (2019)

Rezaee, M., Maleki, V.A.: On the complex mode shapes and natural frequencies of clamped-clamped fluid-conveying pipe. Appl. Ocean Res. **150**, 104113 (2024)

Sapountzakis, E., Dikaros, I.: Non-linear flexural–torsional dynamic analysis of beams of arbitrary cross section by BEM. Int. J. Non-Linear Mech. **46**(5), 782–794 (2011)

Sarparast, H., Ebrahimi-Mamaghani, A., Safarpour, M., Ouakad, H.M., Dimitri, R., Tornabene, F.: Nonlocal study of the vibration and stability response of small-scale axially moving supported beams on viscoelastic-Pasternak foundation in a hygro-thermal environment. Math. Methods Appl. Sci. (2020). https://doi.org/10.1002/mma.6859

Sarvi, P.: The study of the stochastic jump phenomenon in a nonlinear cantilever beam immersed in water under narrow-band random excitation. Aerospace Mechanics **17**(3), 85–95 (2021)

Sobamowo, M., Yinusa, A., Adeleye, O., Oyelade, A., Sadiq, O.: On the analysis of jump and bifurcation phenomena in a forced vibration of geometrical nonlinear cantilever beam: application of differential transformation method. World Sci. News **140**, 26–58 (2020)

Wang, G.-X., Ding, H., Chen, L.-Q.: Dynamic effect of internal resonance caused by gravity on the nonlinear vibration of vertical cantilever beams. J. Sound Vib. **474**, 115265 (2020)

Publisher's Note Springer Nature remains neutral with regard to jurisdictional claims in published maps and institutional affiliations.

Springer Nature or its licensor (e.g. a society or other partner) holds exclusive rights to this article under a publishing agreement with the author(s) or other rightsholder(s); author self-archiving of the accepted manuscript version of this article is solely governed by the terms of such publishing agreement and applicable law.